Original Article

Systematic metabolic profiling of mice with caerulein-induced acute pancreatitis

Linqiang Gong[1#], Shiyuan Zhao[2,3#], Benhui Liang[4], Shanshan Wei[5,6], Yazhou Zhang[7], Shuhui Li[1]^, Hui Yang[8]^, Pei Jiang[2,3]^

[1]Department of Gastroenterology, Tengzhou Central People's Hospital, Tengzhou, China; [2]Translational Pharmaceutical Laboratory, Jining First People's Hospital, Shandong First Medical University, Jining, China; [3]Institute of Translational Pharmacy, Jining Medical Research Academy, Jining, China; [4]Department of Cardiovascular Medicine, Xiangya Hospital, Central South University, Changsha, China; [5]Department of Pharmacy, Shandong Provincial Hospital Affiliated to Shandong First Medical University, Jinan, China; [6]Graduate Department, Shandong First Medical University (Shandong Academy of Medical Sciences), Jinan, China; [7]Department of Foot and Ankle Surgery, Tengzhou Central People's Hospital, Tengzhou, China; [8]Department of Gynecology, Tengzhou Central People's Hospital, Tengzhou, China

Contributions: (I) Conception and design: H Yang, P Jiang; (II) Administrative support: S Li; (III) Provision of study materials or patients: S Wei, Y Zhang; (IV) Collection and assembly of data: S Zhao, B Liang; (V) Data analysis and interpretation: L Gong; (VI) Manuscript writing: All authors; (VII) Final approval of manuscript: All authors.

[#]These authors contributed equally to this work.

Correspondence to: Shuhui Li, MD. Department of Gastroenterology, Tengzhou Central People's Hospital, 181 Xingtan Road, Tengzhou 277599, China. Email: lish9012@126.com; Hui Yang, MD. Department of Gynecology, Tengzhou Central People's Hospital, 181 Xingtan Road, Tengzhou 277599, China. Email: jiayu-1987@163.com; Pei Jiang, PhD. Translational Pharmaceutical Laboratory, Jining First People's Hospital, Shandong First Medical University, Jiankang Road, Jining 272000, China; Institute of Translational Pharmacy, Jining Medical Research Academy, Jining, China. Email: jiangpeicsu@sina.com.

Background: Acute pancreatitis (AP) is a complex inflammatory condition with rising incidence globally. Despite various known causes, early diagnosis remains challenging due to limitations in existing biomarkers. Metabolomics offers a promising avenue for identifying novel biomarkers and elucidating underlying pathophysiological mechanisms. Previous AP metabolomics studies primarily focused on analyzing serum, urine, and pancreatic tissues from patients or animal models. However, systematic metabolomics studies that analyze multiple tissues simultaneously are still lacking. The primary aim of our study is to obtain valuable clues to explore the pathophysiological mechanisms of AP and discover novel biomarkers to enable early detection.

Methods: Using a mouse model of AP induced by cerulein, we conducted gas chromatography-mass spectrometry (GC-MS) metabolomic analysis on serum, pancreas, liver, spleen, colon, and kidney samples. Twelve male C57BL/6J mice were randomly divided into AP and control (CON) groups. Serum and tissue samples were collected, processed, and analyzed using established protocols. Multivariate statistical analysis was employed to identify differential metabolites and impacted metabolic pathways.

Results: Distinct metabolic profiles were observed between AP and CON groups across multiple tissues. Elevated levels of ketone bodies, amino acids, citric acid, and lipids were noted, with significant differences in metabolite levels identified. Notably, 3-hydroxybutyric acid (3-HBA), branched-chain amino acids (BCAAs), phenylalanine, and L-lysine showed consistent alterations, suggesting their potential as early diagnostic biomarkers for AP. Pathway analysis revealed perturbations in several metabolic pathways, providing insights into the pathophysiological mechanisms underlying AP.

Conclusions: Our study highlights the utility of metabolomics in identifying potential biomarkers for early diagnosis of AP and elucidating associated metabolic pathways. 3-HBA, BCAAs, phenylalanine and

^ ORCID: Shuhui Li, 0009-0006-0040-6504; Hui Yang, 0009-0001-6253-357X; Pei Jiang, 0000-0002-8360-7427.

L-lysine emerge as promising biomarkers for further clinical validation. These findings contribute to a better understanding of AP pathophysiology and underscore the potential of metabolomics in precision medicine approaches for AP management.

Keywords: Acute pancreatitis (AP); metabolomics; caerulein; gas chromatography-mass spectrometry (GC-MS); multivariate analysis

Received: 01 February 2024; Accepted: 24 June 2024; Published online: 09 August 2024.
doi: 10.21037/tgh-24-14
View this article at: https://dx.doi.org/10.21037/tgh-24-14

Introduction

Acute pancreatitis (AP) is a prevalent inflammatory condition affecting the pancreas. Well-known causes of AP include gallstones, alcohol, hypertriglyceridemia, hypercalcaemia, drugs, autoimmune diseases, genetic factors, infection, surgical trauma and endoscopic retrograde cholangiopancreatography (ERCP) (1,2). Worldwide, the approximate incidence rate of AP stands at 34 cases per 100,000 person-years (3). With the increasing prevalence of hypertriglyceridemia and metabolic syndrome worldwide, the incidence of AP is on the rise, making the leading cause of gastrointestinal disease-related hospital admissions (4). It is important to note that AP is a complex disease with a variable course, often challenging to predict its stages. Around 80% of patients present with mild to moderately severe AP, which typically resolves within 1 week (5,6). However, about 20% of patients experience severe AP, resulting in a mortality rate ranging from 20% to 40% (5,7). Hence, it is imperative to promptly and precisely identify and diagnose AP.

Although there are several biomarkers available for diagnosing AP, such as serum amylase and lipase, they still have limitations. For instance, serum amylase levels can be within the normal range in patients with alcoholic or hypertriglyceridemia pancreatitis (8,9). Additionally, serum amylase levels or lipase levels can also be elevated in many non-pancreatitis diseases such as bowel perforation, bowel obstruction, bowel infarction, abdominal aortic aneurysm, cholecystitis, biliary obstruction, peptic ulcer disease and acute intestinal pathologies (9). Serum amylase levels in patients with AP typically rise within 6 to 24 hours after onset, while serum lipase levels usually increase within 4 to 8 hours after onset (10). The abdominal computed tomography (CT) manifestations of AP may not be obvious in the early stage, and may even be completely normal (1,10). Therefore, there are no definitive diagnostic biomarkers for early diagnosis of AP, such as within 4 hours. However, due to ethical reasons, early events of AP and studies on new targeted therapies cannot be conducted directly in humans (11). Moreover, the pathophysiology of the AP remains unclear.

The recent development of "omics" technologies has facilitated high-throughput and high-content screening of disease-related biomarkers in biological samples. Metabolomics, in particular, is often employed in biomarker discovery due to its high sensitivity, capable of detecting subtle changes in biological pathways and providing insights into the underlying mechanisms of diseases. Furthermore, metabolomics can provide a more comprehensive understanding of the disease network, as it offers information that is closely related to the pathological or physiological phenotype. Therefore, it has emerged as one of the most promising approaches in precision medicine (12-14).

Highlight box

Key findings

- The metabolic profile resulting from acute pancreatitis (AP) was characterized systematically. 3-hydroxybutyric acid, branched-chain amino acids, phenylalanine, and L-lysine show their potential as early diagnostic biomarkers for AP.

What is known and what is new?

- Previous studies have confirmed that AP is capable of inducing metabolic alterations in serum, urine, and pancreatic tissue.
- A systematic analysis was conducted to examine the metabolic alterations in serum, pancreas, liver, spleen, colon, and kidney induced by AP. The aim was to gain valuable insights into the pathophysiological mechanisms of AP and identify novel biomarkers for early detection.

What is the implication, and what should change now?

- The findings have implications for both research methodology and clinical applications, urging a more integrated and holistic approach in the study and management of AP.

AP can affect other tissues and organs in addition to pancreas, highlighting the need for metabolomic research in other biological samples. However, previous metabolomics studies on AP have primarily focused on analyzing serum, urine, and pancreatic samples from AP patients or animal models, which limits the ability to obtain a complete metabolic profile of the disease. Therefore, a comprehensive and systematic metabolomics analysis of AP is therefore essential. Hence, we adopted a widely used protocol to induce AP in mice (eight intraperitoneal injections of cerulein, each separated by 1 hour, at a dose of 50 μg/kg body weight). Mice were euthanized 1 hour after the last injection, and serum, pancreas, liver, spleen, colon, and kidney were collected for gas chromatography-mass spectrometry (GC-MS) analysis, equivalent to metabolomic analysis 1 hour after onset of AP, in search of differential metabolites that could serve as early diagnostic markers. By detecting alterations in metabolite levels and metabolic pathways, we can gain valuable clues to explore the pathophysiological mechanisms of AP. We present this article in accordance with the ARRIVE reporting checklist (available at https://tgh.amegroups.com/article/view/10.21037/tgh-24-14/rc).

Methods

Animal treatment

Twelve male C57BL/6J mice, each 8 weeks old, sourced from Jinan Pengyue (Jinan, China) were acclimated for a week in a climate-controlled chamber (24±2 ℃, 40% humidity). During this time, they had unrestricted access to both water and food. Subsequently, the mice were randomly divided into two groups: the AP group and the control (CON) group, with each group comprising six mice. All mice underwent a 12-hour fasting period. The AP group received intraperitoneal caerulein injections (50 μg/kg body weight, eight injections at 1-hour intervals) (15), while the mice in the CON group received equivalent injections of normal saline. Euthanasia was performed on all mice 1 hour after the final injection. All experimental procedures followed the Regulations of Experimental Animal Administration set by the State Committee of Science and Technology of the People's Republic of China and received approval from the Ethics Committee of Jining First People's Hospital, Jining, China (No. JNRM-2023-DW-098).

Sample collection and preparation

Anesthesia was initiated by administering sodium pentobarbital via intraperitoneal injection at a dosage of 50 mg/kg. Once anesthetized, blood samples were gathered by removing the eyeballs, followed by centrifugation (3,500 rpm, 8 minutes) to extract serum. Euthanasia was performed on all mice using cervical dislocation. Following this, each mouse underwent necropsy on an ice-cooled surface to retrieve the pancreas, liver, spleen, colon, and kidney. All gathered tissue samples were thoroughly washed with phosphate-buffered saline and promptly frozen in liquid nitrogen. Subsequently, these samples were preserved at –80 ℃ for later use.

For serum sample preparation, a volume of 100 μL of serum was mixed with 350 μL of methanol, incorporating 100 μg/mL of heptadecanoic acid. To collect the supernatant, the resulting mixture was subjected to vortexing and centrifugation (14,000 rpm, 10 minutes, 4 ℃). The collected supernatant was moved to a tube (2 mL) and then dehydrated at 37 ℃ using a nitrogen gas flow. Then, the dried sample was mixed thoroughly with 80 μL of o-methylhydroxylamine hydrochloride, which was dissolved in pyridine at a concentration of 15 mg/mL, and subsequently incubated at 70 ℃ for 90 minutes. Following this step, each sample received an addition of 100 μL of N,O-bis(trimethylsilyl) trifluoroacetamide, including 1% trimethylchlorosilane (Sigma-Aldrich, Saint Louis, MO, USA), followed by an incubation at 70 ℃ lasting 60 minutes. The resulting solution obtained underwent vortexing, followed by centrifugation (14,000 rpm, 2 minutes, 4 ℃), and was subsequently filtered using a 0.22-μm filter before GC-MS analysis. The levels of serum amylase and lipase were assessed through enzymatic kinetic chemistry employing commercial kits within the Roche/Hitachi modular analysis system, following the guidelines outlined by the manufacturer (Roche, Berlin, Germany).

Tissue samples from the pancreas, liver, spleen, colon, and kidney, each weighing 50 mg, underwent homogenization in 1 mL of methanol with 1 mg/mL heptadecanoic acid. Following this, centrifugation (14,000 rpm, 15 minutes, 4 ℃) was performed to obtain the supernatant. More detailed steps regarding further preparation can be referenced in the serum sample preparation description. Quality control samples (QCs) were generated by combining equal amounts of samples from both the CON group and the AP group.

Histopathological staining

The pancreatic tissue underwent fixation in 10% phosphate-buffered paraformaldehyde for 48 hours, followed by embedding in paraffin for histological examination. Sections measuring five microns were sliced utilizing a microtome capable of delivering powerful blows, and subsequently stained employing the hematoxylin-eosin (H&E) technique.

GC-MS analysis

The 7000C mass spectrometer, manufactured by Agilent Technologies (CA, USA), was used to perform all sample analyses in conjunction with a 7890 B gas chromatograph system. The chromatographic analysis employed an HP-5MS capillary column with high-purity helium as the carrier gas, flowing at 1 mL/min with a split ratio of 50:1. Operating temperatures were maintained at 280, 250, and 230 ℃ for injection, transfer line, and ion source, respectively. The gas chromatograph temperature sequence initiated at 60 ℃ for 4 minutes, gradually increasing to 300 ℃ at an 8 ℃/min rate, where it held steady for 5 minutes. The ionization electron impact voltage stood at –70 eV, with a spectra acquisition rate of 20 per second. A full scan mode was employed, covering a scanning range from 50 to 800 m/z.

Multivariate statistical analysis

The GC-MS data underwent initial processing using Agilent Mass Hunter Quantitative Analysis and Unknowns Analysis software, allowing identification of the compounds associated with the detected peaks. Statistical analysis of normalized peak area percentages utilized SIMCA 14.1 software (Umetrics, Sweden). The Orthogonal Projections to Latent Structures Discriminant Analysis (OPLS-DA) model was used to differentiate between the AP group and the CON group. For validation, 200 permutation tests were conducted to assess the validity of the OPLS-DA models.

Two-tailed Student's *t*-tests were performed using SPSS 19.0. Metabolites were considered as potential discriminants if they demonstrated Variable Importance in Projection (VIP) values greater than 1.0 in the OPLS-DA analysis and P values less than 0.05 in the two-tailed Student's *t*-tests. The identified differential metabolites were brought into MetaboAnalyst 5.0 (available at http://www.metaboanalyst.ca) and Kyoto Encyclopedia of Genes and Genomes (KEGG, accessible at http://www.kegg.jp) to perform metabolic pathway analysis. The metabolic pathways that exhibited impact values greater than 0 and P values less than 0.05 were regarded as significantly affected.

Results

Evaluation of caerulein-induced AP in mice

One of the most widely employed models for inducing AP involves administering elevated concentrations of caerulein, an analogue of cholecystokinin (16). Accordingly, our research employed the classical technique of intraperitoneal caerulein injection to induce AP. *Figure 1A*,*1B* illustrated a notable increase in serum amylase and lipase levels within the AP groups. *Figure 1C* depicted representative H&E-stained pancreas images from the AP groups, revealing the infiltration of lymphocytes and neutrophils in the interstitium, accompanied by interstitial edema and a disorganized arrangement of connective tissue. This confirms the successful establishment of caerulein-induced AP mouse models in our study.

GC-MS total ion chromatograms (TICs) of samples

Figure 2 displayed the TICs of QCs. These chromatograms demonstrated robust signal responses across all samples, signifying the identification of a wide range of metabolites with a substantial peak capacity during the analysis. Consistent retention times were noted, and the chromatograms exhibited excellent reproducibility in every tissue.

Multivariate statistical analysis

The OPLS-DA model was utilized to assess the data disparities between the two groups. As evident from the score chart, distinct separation exists between the CON group and the AP group, signifying substantial differences. In order to validate the model, permutation tests were conducted. These tests revealed that the intersections of the regression line for all Q2-points with the left vertical axis were situated below zero, as illustrated in *Figure 3*, suggesting the effectiveness of the model. Cluster analysis focused on the metabolite expression in samples between the two groups, revealing that the majority of samples could be segregated into two separate clusters. There was only a minor overlap observed among the sample clusters (illustrated in *Figure 4*). These findings aligned consistently with the outcomes obtained from the OPLS-DA analysis.

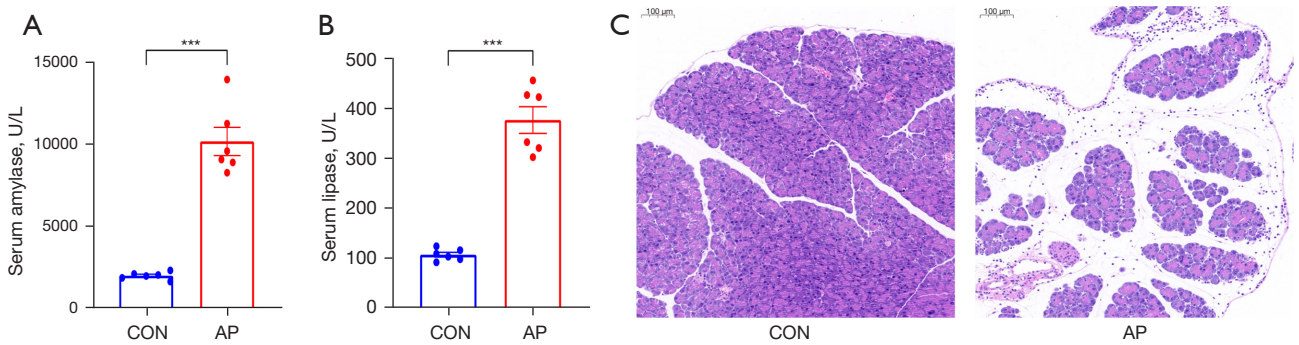

Figure 1 Evaluation of caerulein-induced acute pancreatitis in mice. (A) Serum amylase. (B) Serum lipase. (C) Representative images of pancreatic H&E staining. Values displayed are the mean ± SE, ***, P<0.001 indicates differences between CON and AP groups. CON, control; AP, acute pancreatitis; H&E, hematoxylin and eosin; SE, standard error.

Identification of differential metabolites

Table 1 presented a thorough overview of the distinct metabolites found in specific tissues, namely serum, pancreas, liver, spleen, colon, and kidney. In order to identify significant differences between the CON and AP groups, a threshold was established using VIP values greater than 1.0 and P values lower than 0.05. Metabolites meeting the threshold were determined to be significantly distinct. Moreover, metabolites with a fold change (FC) greater than 1 were classified as displaying an increase, while those with an FC less than 1 were categorized as exhibiting a decrease. It was found that there were 11, 17, 11, 15, 3, and 4 differential metabolites in serum, pancreas, liver, spleen, colon, and kidney, respectively.

Analysis of metabolic pathways

We used MetaboAnalyst 5.0 to explore the metabolic pathways linked to discriminant metabolites. Our analysis revealed 13 impacted metabolic pathways with notable differences (P values <0.05 and impact values >0). Specifically, in serum, the affected pathways involved arginine biosynthesis, glutathione metabolism, and the biosynthesis of phenylalanine, tyrosine, and tryptophan. Moreover, arginine and proline metabolism, as well as D-glutamine and D-glutamate metabolism, were also affected. Within the pancreas, the impacted pathways involved the biosynthesis of phenylalanine, tyrosine, and tryptophan, as well as phenylalanine metabolism. In the liver, the pathways comprised the pentose phosphate pathway, the metabolism of pyrimidine, as well as the biosynthesis of phenylalanine, tyrosine, and tryptophan. In the spleen, the affected pathways involved the metabolism of taurine and hypotaurine, the metabolism of glycerolipids, the metabolism of glutathione, the metabolism of cysteine and methionine, the metabolism of glycine, serine, and threonine, as well as the biosynthesis of phenylalanine, tyrosine, and tryptophan. Meanwhile, the colon included glycerolipid metabolism and sphingolipid metabolism. These affected metabolic pathways were detailed in *Table 2* and visually represented in *Figure 5*. Comprehensive information regarding the impacted metabolic pathways were presented in *Figure 6*.

Discussion

AP is an inflammatory condition affecting the exocrine pancreas, a vital organ involved in both digestion and metabolism. Metabolic diseases such as obesity and hypertriglyceridemia can trigger AP. Of note, AP can also lead to metabolic disorders such as new-onset diabetes, exocrine pancreatic insufficiency (17). This intricate connection underscores the close association between AP and metabolism. Employing untargeted metabolomics, we systematically investigated the alterations in metabolic profiles across serum, pancreas, liver, spleen, colon, and kidney in mice with AP induced by caerulein. Within these tissues, we detected 11 differential metabolites in serum, 17 in the pancreas, 11 in the liver, 15 in the spleen, 3 in the colon, and 4 in the kidney. Among these, significant changes were observed in ketone bodies, amino acids, citric acid, and lipids, indicating their noteworthy alterations.

The serum metabolome represents the final output of all organs and is a detailed systematic characterization

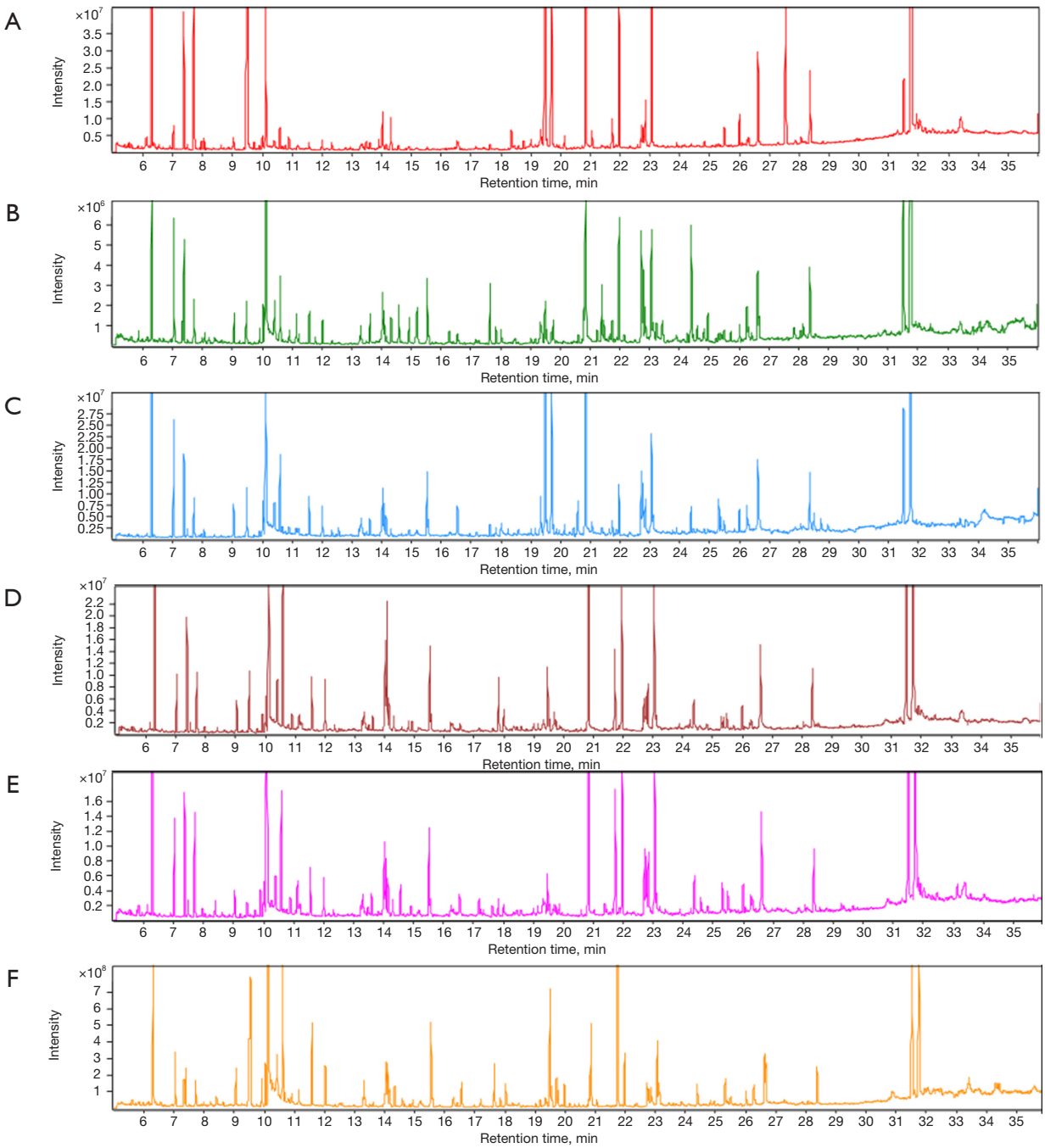

Figure 2 Representative GC-MS total ion current chromatograms from QCs. (A) Serum; (B) pancreas; (C) liver; (D) spleen; (E) colon; (F) kidney (x-axis represents retention time and y-axis represents intensity). GC-MS, gas chromatography-mass spectrometry; QCs, quality control samples.

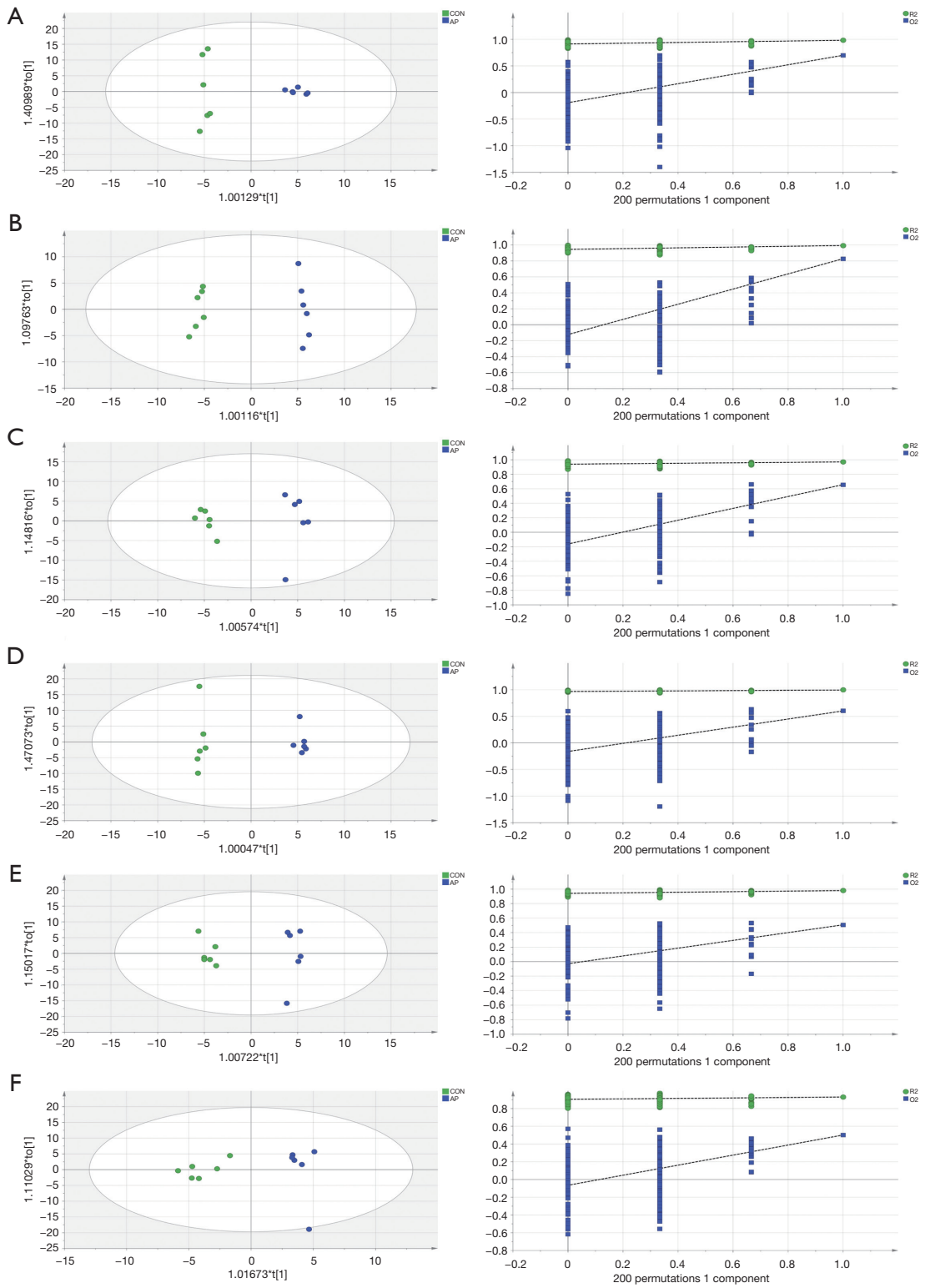

Figure 3 OPLS-DA scores and 200 permutation tests for OPLS-DA models. (A) Serum; (B) pancreas; (C) liver; (D) spleen; (E) colon; (F) kidney. Statistical validation of the significant OPLS-DA models by permutation tests revealed no over-fitting (note that the blue regression line of the Q2 points intersect the vertical axis at values <0). OPLS-DA, Orthogonal Projections to Latent Structures Discriminant Analysis; CON, control; AP, acute pancreatitis.

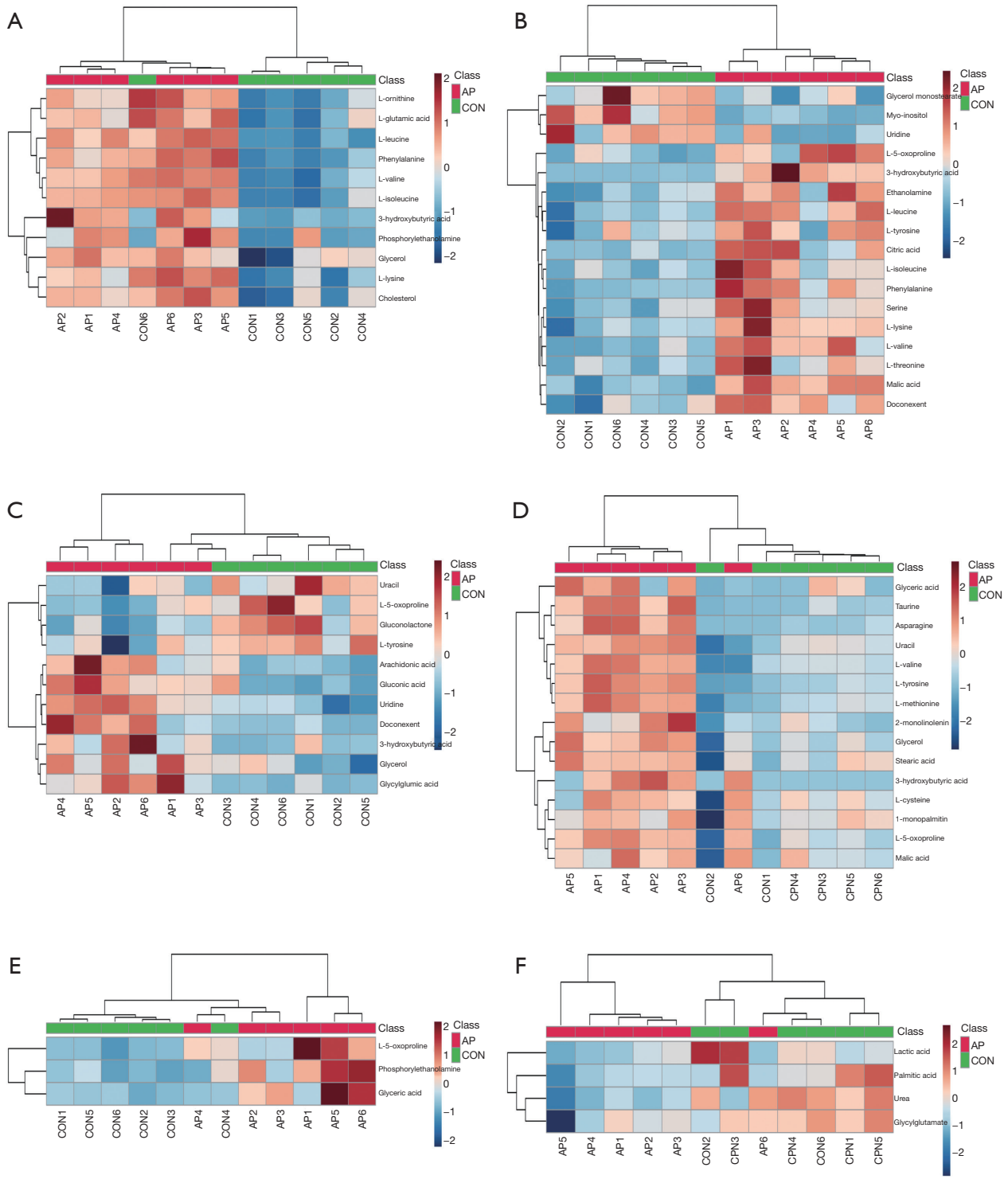

Figure 4 Heatmap illustrating variance in metabolites between AP and CON groups. (A) Serum; (B) pancreas; (C) liver; (D) spleen; (E) colon; (F) kidney. Red and blue colors denote upregulation and downregulation, respectively. Rows and columns correspond to metabolites and samples, respectively. AP, acute pancreatitis; CON, control.

Table 1 Differential metabolites identified in the serum, pancreas, liver, spleen, colon, and kidney between AP and CON groups

Metabolites	HMDB	VIP	P	Fold change
Serum				
3-hydroxybutyric acid	HMDB0000357	1.81	4.25E−04	5.37
L-valine	HMDB0000883	1.58	5.82E−03	2.31
L-lysine	HMDB0000182	1.46	1.87E−02	2.36
L-ornithine	HMDB0000214	1.24	4.29E−02	2.32
L-glutamic acid	HMDB0000148	1.22	4.47E−02	2.03
L-leucine	HMDB0000687	1.89	4.00E−03	4.01
Phosphorylethanolamine	HMDB0000224	1.78	9.00E−03	2.62
Phenylalanine	HMDB0000159	1.73	9.00E−03	3.25
L-isoleucine	HMDB0000172	1.67	1.50E−02	2.48
Cholesterol	HMDB0000067	1.59	4.00E−03	1.90
Glycerol	HMDB0000131	1.26	2.60E−02	1.52
Pancreas				
Malic acid	HMDB0000744	1.91	2.47E−05	1.85
Myo-inositol	HMDB0000211	1.82	3.44E−04	0.46
L-valine	HMDB0000883	1.77	5.78E−04	2.07
L-leucine	HMDB0000687	1.64	3.35E−03	1.93
Ethanolamine	HMDB0000149	1.60	4.02E−03	1.96
Doconexent	HMDB0002183	1.52	4.87E−03	1.54
Serine	HMDB0062263	1.50	8.59E−03	1.70
L-5-oxoproline	HMDB0000267	1.40	1.01E−02	1.54
L-threonine	HMDB0000167	1.38	1.88E−02	1.64
L-isoleucine	HMDB0000172	1.41	1.96E−02	1.98
Glycerol monostearate	HMDB0011535	1.35	3.54E−02	0.81
L-tyrosine	HMDB0000158	1.18	4.82E−02	1.34
Phenylalanine	HMDB0000159	1.78	2.00E−03	1.93
3-hydroxybutyric acid	HMDB0000357	1.69	2.00E−03	4.25
Citric acid	HMDB0000094	1.58	9.00E−03	4.78
L-lysine	HMDB0000182	1.58	2.00E−03	1.98
Uridine	HMDB0000296	1.33	4.10E−02	0.66
Liver				
Uridine	HMDB0000296	1.89	1.00E−03	2.04
Gluconolactone	HMDB0000150	1.87	3.00E−03	0.33
Arachidonic acid	HMDB0001043	1.71	1.30E−02	1.46
Glycerol	HMDB0000131	1.44	2.50E−02	1.28

Table 1 (*continued*)

Table 1 (*continued*)

Metabolites	HMDB	VIP	P	Fold change
Uracil	HMDB0000300	1.39	2.90E−02	0.74
L-tyrosine	HMDB0000158	1.45	3.90E−02	0.63
L-5-oxoproline	HMDB0000267	1.41	4.60E−02	0.67
Doconexent	HMDB0002183	1.82	4.00E−03	1.51
Gluconic acid	HMDB0000625	1.77	2.60E−02	1.58
Glycylglutamic acid	HMDB0028840	1.60	4.00E−03	1.89
3-hydroxybutyric acid	HMDB0000357	1.49	1.50E−02	1.65
Spleen				
L-5-oxoproline	HMDB0000267	1.63	2.00E−03	1.98
Glycerol	HMDB0000131	1.58	6.00E−03	1.92
L-tyrosine	HMDB0000158	1.43	1.30E−02	3.06
2-monolinolenin	HMDB0011540	1.47	1.60E−02	2.37
L-methionine	HMDB0000696	1.38	1.80E−02	2.12
Stearic acid	HMDB0000827	1.33	2.60E−02	1.65
Malic acid	HMDB0000744	1.30	3.20E−02	1.66
3-hydroxybutyric acid	HMDB0000357	1.70	1.50E−02	45.57
Taurine	HMDB0000251	1.56	4.10E−02	5.44
Asparagine	HMDB0000168	1.54	2.60E−02	7.59
Uracil	HMDB0000300	1.17	4.10E−02	1.68
L-valine	HMDB0000883	1.12	4.10E−02	1.90
Glyceric acid	HMDB0000139	1.10	2.60E−02	2.63
L-cysteine	HMDB0000574	1.06	4.10E−02	1.48
1-monopalmitin	HMDB0011564	1.01	4.10E−02	1.39
Colon				
Phosphorylethanolamine	HMDB0000224	1.77	3.20E−02	3.63
Glyceric acid	HMDB0000139	1.94	2.60E−02	4.10
L-5-oxoproline	HMDB0000267	1.80	9.00E−03	2.11
Kidney				
Urea	HMDB0000294	1.52	2.80E−02	0.50
Palmitic acid	HMDB0000220	2.13	1.50E−02	0.65
Lactic acid	HMDB0000190	1.86	1.50E−02	0.70
Glycyl glutamate	HMDB0028840	1.34	2.60E−02	0.71

AP, acute pancreatitis; CON, control; HMDB, Human Metabolome Database; VIP, Variable Importance in Projection.

Table 2 Specifics concerning differential metabolic pathways across different tissues

Tissue	Pathway name	Match status	Hits	P	Impact
Serum	Arginine biosynthesis	2/14	L-glutamate; L-ornithine	4.21E–03	1.78E–01
	Glutathione metabolism	2/28	L-glutamate; L-ornithine	1.65E–02	1.97E–02
	Phenylalanine, tyrosine and tryptophan biosynthesis	1/4	L-phenylalanine	2.89E–02	5.00E–01
	Arginine and proline metabolism	2/38	L-glutamate; L-ornithine	2.95E–02	1.97E–01
	D-glutamine and D-glutamate metabolism	1/6	L-glutamate	4.31E–02	5.00E–01
Pancreas	Phenylalanine, tyrosine and tryptophan biosynthesis	2/4	L-phenylalanine; L-tyrosine	4.77E–04	1.00E+00
	Phenylalanine metabolism	2/12	L-phenylalanine; L-tyrosine	5.02E–03	3.57E–01
Liver	Pentose phosphate pathway	2/22	D-gluconic acid; D-glucono-1,5-lactone	8.54E–03	4.71E–02
	Pyrimidine metabolism	2/39	Uridine; uracil	2.58E–02	9.01E–02
	Phenylalanine, tyrosine and tryptophan biosynthesis	1/4	L-tyrosine	2.63E–02	5.00E–01
Spleen	Taurine and hypotaurine metabolism	2/8	L-cysteine; taurine	1.59E–03	4.29E–01
	Glycerolipid metabolism	2/16	Glycerol; D-glycerate	6.57E–03	3.30E–01
	Glutathione metabolism	2/28	L-cysteine; 5-oxoproline	1.96E–02	1.05E–02
	Cysteine and methionine metabolism	2/33	L-methionine; L-cysteine	2.68E–02	2.00E–01
	Glycine, serine and threonine metabolism	2/34	D-glycerate; L-cysteine	2.83E–02	2.25E–02
	Phenylalanine, tyrosine and tryptophan biosynthesis	1/4	L-tyrosine	3.15E–02	5.00E–01
Colon	Glycerolipid metabolism	1/16	D-glycerate	3.16E–02	9.35E–02
	Sphingolipid metabolism	1/21	Ethanolamine phosphate	4.13E–02	1.42E–02

of physiological state or pathological condition. In our study, 11 differential metabolites were detected in serum, these differential metabolites may be used as potential biomarkers, may be helpful for the early diagnosis of AP. The differential metabolites most likely to be potential biomarkers are discussed in detail in the following article.

3-Hydroxybutyric acid (3-HBA), categorized among ketone bodies, is an important metabolite of AP. We discovered serum 3-HBA levels were significantly elevated in AP mice, consistent with previous studies (18-20). Elevated levels of 3-HBA in serum due to AP are caused and maintained by significantly high levels of pancreatic lipase in the bloodstream (21). In the course of AP, the improper release of pancreatic lipase can lead to both self-digestion of the pancreas and excessive breakdown of adipose tissues (22-24). If uncontrolled, this process will generate an overwhelming quantity of nonesterified fatty acids (NEFAs), which further damage pancreatic acinar cells and potentially lead to organ failure (22,23,25). It is well known that fatty acid β-oxidation (FAO), a principal catabolic process, breaks down NEFAs into acetyl-CoA (26), which can then be used for energy production through the tricarboxylic acid (TCA) cycle or ketogenesis. The liver, highly active in FAO, also serves as a primary site for synthesizing ketone bodies. Of note, both human and experimental animal models of AP have shown activation of hepatic FAO and ketogenesis processes (27). These analyses might explain the elevated levels of 3-HBA. Initially, there was a belief that excessive production of ketone bodies might result in harmful conditions like ketoacidosis or ketonemia. Significantly, a recent study discovered that 3-HBA significantly diminished the activation of pancreatic and systemic proinflammatory macrophages, assuming an inherent protective role during AP (27). Furthermore, our study identified increased levels

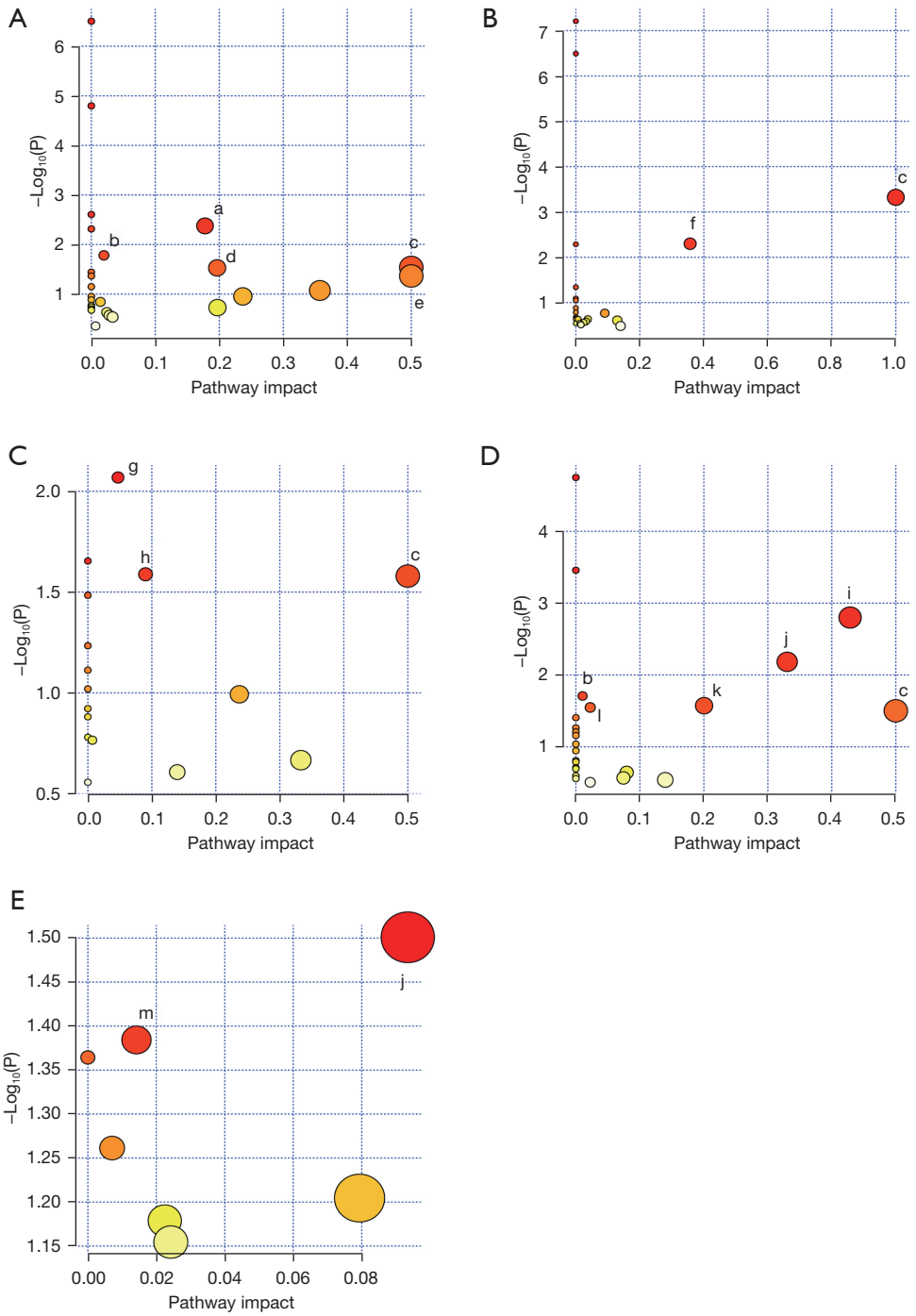

Figure 5 Summary of differential metabolic pathways using MetaboAnalyst 5.0. The node color is based on the P values (y axis) and the node radius represents the pathway impact values (x axis). (A) Serum; (B) pancreas; (C) liver; (D) spleen; (E) colon. (a) Arginine biosynthesis; (b) glutathione metabolism; (c) phenylalanine, tyrosine and tryptophan biosynthesis; (d) arginine and proline metabolism; (e) D-glutamine and D-glutamate metabolism; (f) phenylalanine metabolism; (g) pentose phosphate pathway; (h) pyrimidine metabolism; (i) taurine and hypotaurine metabolism; (j) glycerolipid metabolism; (k) cysteine and methionine metabolism; (l) glycine, serine and threonine metabolism; (m) sphingolipid metabolism.

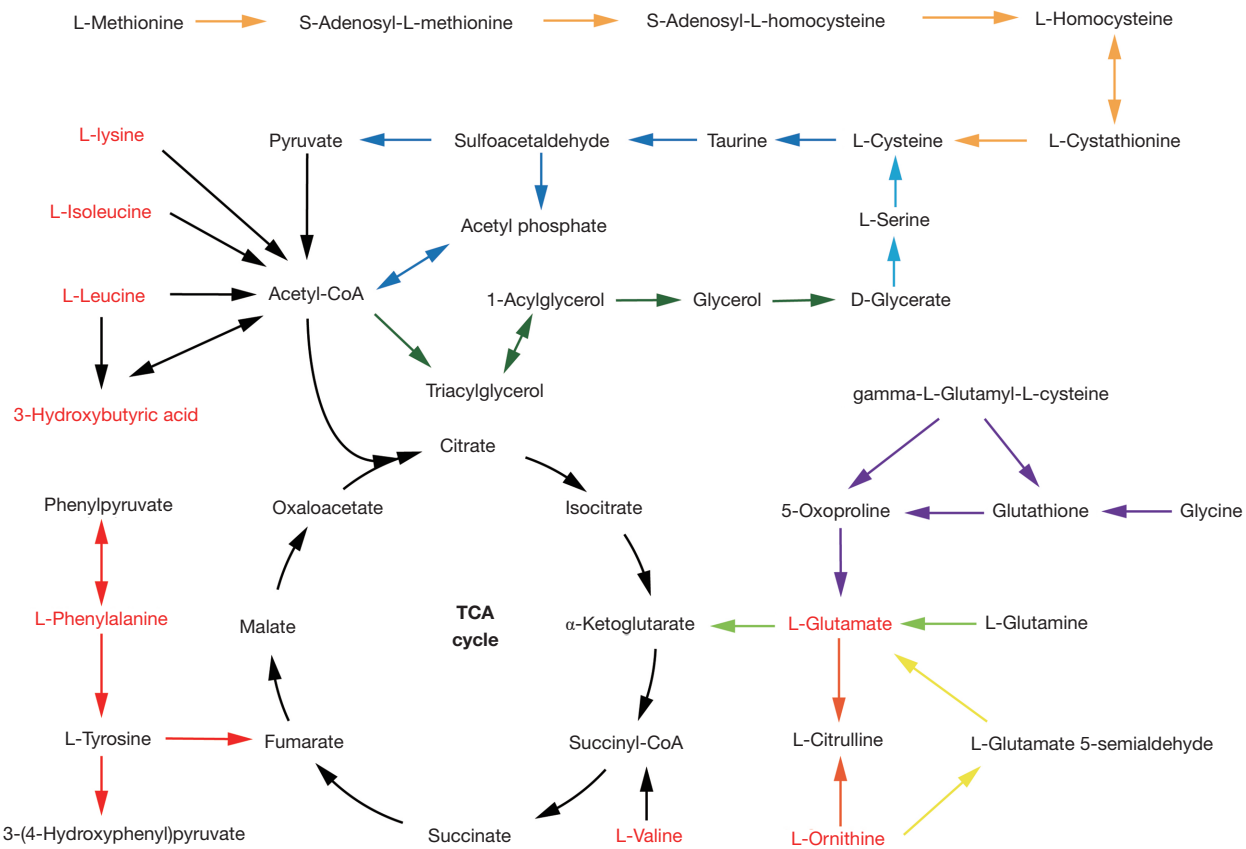

Figure 6 Schematic diagram of related differential metabolic pathways affected by AP. Black arrows indicate energy metabolism pathways, including the tricarboxylic acid cycle. Deep red arrows indicate phenylalanine, tyrosine, and tryptophan biosynthesis. Red arrows indicate arginine biosynthesis. Golden arrows indicate arginine and proline metabolism. Light green arrows indicate L-glutamine and L-glutamate metabolism. Blue arrows indicate taurine and hypotaurine metabolism. Green arrows indicate glycerolipid metabolism. Purple arrows indicate glutathione metabolism. Dark orange arrows indicate cysteine and methionine metabolism. Light blue arrows indicate glycine, serine and threonine metabolism. Metabolites marked in red represent potential biomarkers identified in the study. TCA, tricarboxylic acid; AP, acute pancreatitis.

of 3-HBA in the pancreas, liver, and spleen. Consequently, 3-HBA shows promise as a potential biomarker for AP (18).

Besides the rise in 3-HBA, heightened levels of branched-chain amino acids (BCAAs) were noted in both serum and pancreatic tissue of mice with caerulein-induced AP, consistent with findings from previous studies involving AP patients or murine models (28,29). BCAAs, a group of three essential amino acids: leucine, isoleucine, and valine, are crucial for maintaining regular pancreatic enzyme functions (30). Earlier proteomic investigations of AP revealed a decrease in the breakdown of BCAAs during the condition (31,32). Additionally, AP has been observed to induce alterations in gut microbiota (33,34). Specifically, AP presents a distinct gut microbial profile characterized by reduced microbial diversity, increased presence of pathogenic bacteria, and diminished levels of beneficial bacteria (35-37). BCAAs are synthesized by various sources such as plants, fungi, and bacteria, notably by members of the gut microbiota (38). We propose that shifts in gut microbiota in AP patients or animal models could influence BCAA synthesis, warranting further studies to confirm this hypothesis. These analyses might explain the increased levels of BCAAs detected in serum and pancreatic tissues during AP. Now, the question arises: what is the significance of these elevated BCAAs? BCAAs play a critical role in maintaining mammalian homeostasis by regulating immunity (39). An intriguing recent study suggested that a high BCAA diet could reduce inflammatory levels in

mice with Parkinson's disease (40). Therefore, whether the increased levels of BCAAs might exhibit an anti-inflammatory role in AP. To validate this hypothesis, further research is essential. Consequently, BCAAs shows promise as potential biomarkers for AP.

Consistent with prior research (20,41), the levels of phenylalanine in serum were also elevated in AP mice. AP typically commences as localized sterile inflammation and can potentially advance to systemic inflammatory response syndrome (SIRS). Infections or states of inflammation often lead to considerable rises in serum phenylalanine (42). Therefore, phenylalanine can be considered as a biomarker for early diagnosis of AP.

In our study, we observed substantial elevations in tyrosine levels in the pancreas and spleen. Interestingly, a recent study highlighted that the microbial metabolism of L-tyrosine provided protection against allergic airway inflammation and was also effective against neutrophilic inflammation (43). Therefore, we propose that the heightened tyrosine levels might indicate the body's compensatory anti-inflammatory responses. Nevertheless, further research is necessary to validate this hypothesis.

The levels of L-lysine in serum and pancreas of AP mice were elevated significantly compared with CON group. Previous research has confirmed that L-lysine administration caused early pancreatic mitochondrial damage, may lead to the development of AP (44). Therefore, L-lysine can be considered as a biomarker for early diagnosis of AP.

Consistent with a preceding study (45), there was a notable elevation in the level of citric acid observed within the pancreas of caerulein-induced AP mice models. Pancreatitis disrupts the equilibrium of Ca^{2+}, leading to a notable rise in Ca^{2+} concentration within pancreatic acinar cells (46). The excessive increase in cellular concentration of Ca^{2+} induces the activation of the mitochondrial permeability transition pore (MPTP), causing the depletion of crucial mitochondrial membrane potential necessary for adenosine triphosphate (ATP) synthesis (47,48). Taken together, pancreatic acinar cells exhibit mitochondrial dysfunction and decreased ATP production during AP (47,49,50). Our hypothesis suggests that the TCA cycle, responsible for generating energy within the mitochondria of pancreatic acinar cells during pancreatitis, is highly likely to be affected. This may elucidate the rise in citric acid, an essential intermediate of the TCA cycle, observed in the pancreas during pancreatitis. It is worth noting that citric acid accumulation in macrophages serves distinct nonmetabolic signaling roles influencing inflammatory gene expression during the activation of proinflammatory macrophages (51). However, it remains uncertain whether citric acid within pancreatic acinar cells also participates in signaling processes within the inflammatory pathway, necessitating further studies to explore this potential aspect.

Although our study yielded valuable insights, it is important to recognize certain limitations that persist. Metabolic profiling of caerulein-induced AP mice in only one time point may be accidental. In the further, we will design this study at several time points, instead of one time point, which help to understand the changes in metabolites. Also, additional clinical studies are needed to determine whether these biomarkers are applicable to humans. Metabolomics is the only omics approach we have used to study AP. To ensure the credibility of our findings, it is crucial to incorporate various methodologies comprising genomics, transcriptomics, proteomics, and metabolomics. Many metabolites exhibit short lifespans, and our study involves gathering samples from multiple tissues, a task that is time-consuming and challenging to entirely avoid. This circumstance may potentially impact the accuracy of the final measurement of metabolites. Additionally, it is crucial to acknowledge that anesthesia used during sampling procedures can trigger metabolic shifts in tissues, potentially influencing the outcomes (52).

Conclusions

Utilizing GC-MS and multivariate statistical analysis, we discerned systematic metabolic alterations induced by AP. Many differential metabolites in serum, pancreas, liver, spleen, colon, and kidney were identified, primarily comprising ketone bodies, amino acids, lipids, and intermediates of the TCA cycle. These metabolites were chiefly associated with amino acid and glycerolipid metabolism. Notably, 3-HBA, BCAAs, phenylalanine and L-lysine emerge as promising biomarkers for early diagnosis of AP. Recent research has unveiled non-metabolic functions for specific metabolites (e.g., 3-HBA, BCAAs, L-tyrosine, citric acid), indicating their roles in regulating inflammatory processes. Furthermore, gut microbiota significantly influences metabolite synthesis and contributes to the progression of AP. Further investigations are imperative to unravel the intricate connections between metabolites, gut microbiota, and AP, potentially offering a new perspective on its pathogenesis.

Acknowledgments

Funding: This research was funded by the National Natural Science Foundation of China (Nos. 81602846 and 82272253), Natural Science Foundation of Shandong Province (No. ZR2021MH145), Taishan Scholar Project of Shandong Province (No. tsqn201812159), Science and Technology Program of Traditional Chinese Medicine of Shandong Province (No. M-2022066), and China International Medical Foundation (No. Z-2018-35-2002).

Footnote

Reporting Checklist: The authors have completed the ARRIVE reporting checklist. Available at https://tgh.amegroups.com/article/view/10.21037/tgh-24-14/rc

Data Sharing Statement: Available at https://tgh.amegroups.com/article/view/10.21037/tgh-24-14/dss

Peer Review File: Available at https://tgh.amegroups.com/article/view/10.21037/tgh-24-14/prf

Conflicts of Interest: All authors have completed the ICMJE uniform disclosure form (available at https://tgh.amegroups.com/article/view/10.21037/tgh-24-14/coif). The authors have no conflicts of interest to declare.

Ethical Statement: The authors are accountable for all aspects of the work in ensuring that questions related to the accuracy or integrity of any part of the work are appropriately investigated and resolved. All experimental procedures followed the Regulations of Experimental Animal Administration set by the State Committee of Science and Technology of the People's Republic of China and received approval from the Ethics Committee of Jining First People's Hospital, Jining, China (No. JNRM-2023-DW-098).

References

1. Banks PA, Bollen TL, Dervenis C, et al. Classification of acute pancreatitis--2012: revision of the Atlanta classification and definitions by international consensus. Gut 2013;62:102-11.
2. Boxhoorn L, Voermans RP, Bouwense SA, et al. Acute pancreatitis. Lancet 2020;396:726-34.
3. Xiao AY, Tan ML, Wu LM, et al. Global incidence and mortality of pancreatic diseases: a systematic review, meta-analysis, and meta-regression of population-based cohort studies. Lancet Gastroenterol Hepatol 2016;1:45-55.
4. Iannuzzi JP, King JA, Leong JH, et al. Global Incidence of Acute Pancreatitis Is Increasing Over Time: A Systematic Review and Meta-Analysis. Gastroenterology 2022;162:122-34.
5. Forsmark CE, Vege SS, Wilcox CM. Acute Pancreatitis. N Engl J Med 2016;375:1972-81.
6. Krishna SG, Kamboj AK, Hart PA, et al. The Changing Epidemiology of Acute Pancreatitis Hospitalizations: A Decade of Trends and the Impact of Chronic Pancreatitis. Pancreas 2017;46:482-8.
7. Lankisch PG, Apte M, Banks PA. Acute pancreatitis. Lancet 2015;386:85-96.
8. Al-Bahrani AZ, Ammori BJ. Clinical laboratory assessment of acute pancreatitis. Clin Chim Acta 2005;362:26-48.
9. Tenner S, Baillie J, DeWitt J, et al. American College of Gastroenterology guideline: management of acute pancreatitis. Am J Gastroenterol 2013;108:1400-15; 1416.
10. Vissers RJ, Abu-Laban RB, McHugh DF. Amylase and lipase in the emergency department evaluation of acute pancreatitis. J Emerg Med 1999;17:1027-37.
11. Silva-Vaz P, Abrantes AM, Castelo-Branco M, et al. Murine Models of Acute Pancreatitis: A Critical Appraisal of Clinical Relevance. Int J Mol Sci 2019;20:2794.
12. Long NP, Nghi TD, Kang YP, et al. Toward a Standardized Strategy of Clinical Metabolomics for the Advancement of Precision Medicine. Metabolites 2020;10:51.
13. Johnson CH, Ivanisevic J, Siuzdak G. Metabolomics: beyond biomarkers and towards mechanisms. Nat Rev Mol Cell Biol 2016;17:451-9.
14. Bjerrum JT, Nielsen OH. Metabonomics in Gastroenterology and Hepatology. Int J Mol Sci 2019;20:3638.
15. Lei Y, Tang L, Liu S, et al. Parabacteroides produces acetate to alleviate heparanase-exacerbated acute pancreatitis through reducing neutrophil infiltration.

Microbiome 2021;9:115.
16. Lerch MM, Gorelick FS. Models of acute and chronic pancreatitis. Gastroenterology 2013;144:1180-93.
17. Petrov MS, Olesen SS. Metabolic Sequelae: The Pancreatitis Zeitgeist of the 21st Century. Gastroenterology 2023;165:1122-35.
18. Xiao H, Huang JH, Zhang XW, et al. Identification of potential diagnostic biomarkers of acute pancreatitis by serum metabolomic profiles. Pancreatology 2017;17:543-9.
19. Bohus E, Coen M, Keun HC, et al. Temporal metabonomic modeling of l-arginine-induced exocrine pancreatitis. J Proteome Res 2008;7:4435-45.
20. Guo J, Li X, Wang D, et al. Exploring metabolic biomarkers and regulation pathways of acute pancreatitis using ultra-performance liquid chromatography combined with a mass spectrometry-based metabolomics strategy. RSC Adv 2019;9:12162-73.
21. Kabadi UM. Pancreatic ketoacidosis: ketonemia associated with acute pancreatitis. Postgrad Med J 1995;71:32-5.
22. Navina S, Acharya C, DeLany JP, et al. Lipotoxicity causes multisystem organ failure and exacerbates acute pancreatitis in obesity. Sci Transl Med 2011;3:107ra110.
23. de Oliveira C, Khatua B, Noel P, et al. Pancreatic triglyceride lipase mediates lipotoxic systemic inflammation. J Clin Invest 2020;130:1931-47.
24. Noel P, Patel K, Durgampudi C, et al. Peripancreatic fat necrosis worsens acute pancreatitis independent of pancreatic necrosis via unsaturated fatty acids increased in human pancreatic necrosis collections. Gut 2016;65:100-11.
25. Khatua B, El-Kurdi B, Patel K, et al. Adipose saturation reduces lipotoxic systemic inflammation and explains the obesity paradox. Sci Adv 2021;7:eabd6449.
26. Rinaldo P, Matern D, Bennett MJ. Fatty acid oxidation disorders. Annu Rev Physiol 2002;64:477-502.
27. Zhang L, Shi J, Du D, et al. Ketogenesis acts as an endogenous protective programme to restrain inflammatory macrophage activation during acute pancreatitis. EBioMedicine 2022;78:103959.
28. Wang R, Wang Y, Tao Y, et al. Temporal Proteomic and Lipidomic Profiles of Cerulein-Induced Acute Pancreatitis Reveal Novel Insights for Metabolic Alterations in the Disease Pathogenesis. ACS Omega 2023;8:12310-26.
29. Peng Y, Hong J, Raftery D, et al. Metabolomic-based clinical studies and murine models for acute pancreatitis disease: A review. Biochim Biophys Acta Mol Basis Dis 2021;1867:166123.
30. Lyman RL, Wilcox SS. Effect of acute amino acid deficiencies on carcass composition and pancreatic function in the force-fed rat. II. Deficiencies of valine, lysine, tryptophan, leucine and isoleucine. J Nutr 1963;79:37-44.
31. Wang C, Zhang Y, Tan J, et al. Improved Integrated Whole Proteomic and Phosphoproteomic Profiles of Severe Acute Pancreatitis. J Proteome Res 2020;19:2471-82.
32. García-Hernández V, Sánchez-Bernal C, Schvartz D, et al. A tandem mass tag (TMT) proteomic analysis during the early phase of experimental pancreatitis reveals new insights in the disease pathogenesis. J Proteomics 2018;181:190-200.
33. Pan LL, Li BB, Pan XH, et al. Gut microbiota in pancreatic diseases: possible new therapeutic strategies. Acta Pharmacol Sin 2021;42:1027-39.
34. Chen J, Huang C, Wang J, et al. Dysbiosis of intestinal microbiota and decrease in paneth cell antimicrobial peptide level during acute necrotizing pancreatitis in rats. PLoS One 2017;12:e0176583.
35. Tao X, Guo F, Zhou Q, et al. Bacterial community mapping of the intestinal tract in acute pancreatitis rats based on 16S rDNA gene sequence analysis. RSC Adv 2019;9:5025-36.
36. Brubaker L, Luu S, Hoffman K, et al. Microbiome changes associated with acute and chronic pancreatitis: A systematic review. Pancreatology 2021;21:1-14.
37. Zhou Q, Tao X, Guo F, et al. Tryptophan metabolite norharman secreted by cultivated Lactobacillus attenuates acute pancreatitis as an antagonist of histone deacetylases. BMC Med 2023;21:329.
38. Agus A, Clément K, Sokol H. Gut microbiota-derived metabolites as central regulators in metabolic disorders. Gut 2021;70:1174-82.
39. Tajiri K, Shimizu Y. Branched-chain amino acids in liver diseases. Transl Gastroenterol Hepatol 2018;3:47.
40. Yan Z, Yang F, Sun L, et al. Role of gut microbiota-derived branched-chain amino acids in the pathogenesis of Parkinson's disease: An animal study. Brain Behav Immun 2022;106:307-21.
41. Sandstrom P, Trulsson L, Gasslander T, et al. Serum amino acid profile in patients with acute pancreatitis. Amino Acids 2008;35:225-31.
42. Wannemacher RW Jr, Klainer AS, Dinterman RE, et al. The significance and mechanism of an increased serum phenylalanine-tyrosine ratio during infection. Am J Clin Nutr 1976;29:997-1006.
43. Wypych TP, Pattaroni C, Perdijk O, et al. Microbial metabolism of L-tyrosine protects against allergic airway inflammation. Nat Immunol 2021;22:279-86.
44. Biczó G, Hegyi P, Dósa S, et al. The crucial role of

early mitochondrial injury in L-lysine-induced acute pancreatitis. Antioxid Redox Signal 2011;15:2669-81.
45. Sakai A, Nishiumi S, Shiomi Y, et al. Metabolomic analysis to discover candidate therapeutic agents against acute pancreatitis. Arch Biochem Biophys 2012;522:107-20.
46. Maléth J, Hegyi P. Ca2+ toxicity and mitochondrial damage in acute pancreatitis: translational overview. Philos Trans R Soc Lond B Biol Sci 2016;371:20150425.
47. Mukherjee R, Mareninova OA, Odinokova IV, et al. Mechanism of mitochondrial permeability transition pore induction and damage in the pancreas: inhibition prevents acute pancreatitis by protecting production of ATP. Gut 2016;65:1333-46.
48. Halestrap AP, Richardson AP. The mitochondrial permeability transition: a current perspective on its identity and role in ischaemia/reperfusion injury. J Mol Cell Cardiol 2015;78:129-41.
49. Shalbueva N, Mareninova OA, Gerloff A, et al. Effects of oxidative alcohol metabolism on the mitochondrial permeability transition pore and necrosis in a mouse model of alcoholic pancreatitis. Gastroenterology 2013;144:437-446.e6.
50. Biczo G, Vegh ET, Shalbueva N, et al. Mitochondrial Dysfunction, Through Impaired Autophagy, Leads to Endoplasmic Reticulum Stress, Deregulated Lipid Metabolism, and Pancreatitis in Animal Models. Gastroenterology 2018;154:689-703.
51. Ryan DG, O'Neill LAJ. Krebs Cycle Reborn in Macrophage Immunometabolism. Annu Rev Immunol 2020;38:289-313.
52. Jang C, Chen L, Rabinowitz JD. Metabolomics and Isotope Tracing. Cell 2018;173:822-37.

doi: 10.21037/tgh-24-14
Cite this article as: Gong L, Zhao S, Liang B, Wei S, Zhang Y, Li S, Yang H, Jiang P. Systematic metabolic profiling of mice with caerulein-induced acute pancreatitis. Transl Gastroenterol Hepatol 2024;9:65.